Int J Clin Exp Med 2021;14(1):105-116
www.ijcem.com /ISSN:1940-5901/IJCEM0110849

Original Article

The expressions and clinical value of miR-155 and miR-34a in purulent lymphadenitis in children

Meng Qi[1], Xin Li[2], Libao Sun[1], Jianda Wang[1]

[1]*Department of Pediatric Surgery, Maternity and Child Care Center of Qinhuangdao, Qinhuangdao Maternal and Child Health Hospital, Qinhuangdao 066000, Hebei, People's Republic of China;* [2]*Department of Oncology, Qinhuangdao Haigang Hospital, Qinhuangdao 066000, Hebei, People's Republic of China*

Received March 14, 2020; Accepted May 22, 2020; Epub January 15, 2021; Published January 30, 2021

Abstract: Objective: To explore the expressions and clinical value of miR-155 and miR-34a in children with purulent lymphadenitis. Methodology: Altogether 50 cases of lymph node lumps and 50 cases of healthy adjacent tissues were collected from children with purulent lymphadenitis from March 2017 to March 2019 in our hospital for this retrospective study. At the same time, human lymphocyte B lymphocyte Pfeiffer cells were transfected and double luciferase experiments were carried out. The miR-155 and miR-34a expression levels and the SHIP1 and RCAN1 mRNA and protein expression levels in the lumps and healthy tissues were measured, and the mRNA and protein levels of the patients with different clinical symptoms were compared. The proliferation and apoptosis of the cells over-expressing miR-155 and miR-34a were measured. Results: The miR-155 and miR-34a expression levels were higher in the lump tissues, but the SHIP1 and RCAN1 mRNA protein expression levels were lower. The miR-155 and miR-34a expression levels were higher in the lumps > 3 cm, higher in the patients with a moderate or high fever, and lower in the mRNA protein expression levels of the corresponding SHIP1 and RCAN1. At the same time, miR-155 had a targeted inhibitory effect on SHIP1, and miR-34a had a targeted inhibitory effect on RCAN1. When miR-155 and miR-34a were over-expressed, the growth of two groups of cells became faster and the apoptosis slowed down. The miR-155 and miR-34a expressions in children with purulent lymphadenitis increase. The targeted inhibition of SHIP1 and RCAN1 aggravates the inflammatory reaction, which leads to an enlargement of the lymphoid lumps.

Keywords: miR-155, miR-34a, SHIP1, RCAN1, purulent lymphadenitis in children

Introduction

Purulent lymphadenitis is a very challenging disease. It mostly occurs in children, with nearly 90% of cases affecting children aged 4-8 [1-3]. This disease is generally caused by microbial infection sources such as bacteria and viruses, of which group A Streptococcus and *Staphylococcus aureus* are common pathogens [4]. At the same time, lymphadenitis is also a complication caused by some vaccines such as Bacillus Calmette-Guerin Vaccine (BCG) injection [5, 6]. The symptoms of this disease include a thinning and whitening of the skin, painless cervical lymph node lumps ranging in size from 1 cm to 6 cm [7-9] and which slowly expand. The disease is very harmful to children's health.

Fine needle aspiration, surgical resection, and antibiotics were commonly used to treat purulent lymphadenitis in the past. However, such methods not only easily produce drug resistance to pathogens, they also easily cause scars on patients [10, 11]. In recent years, the targeting effect of microRNA has attracted people's attention. It can regulate mRNA by binding to the 3'-untranslated region (3'-UTR) of target mRNA and can further regulate gene expression. Abnormal expression levels of it easily cause diseases [12, 13]. Related studies have found that miR-155 exists as a carcinogen in lymphoma [14], and miR-155 expression is upregulated in some types of inflammation [15]. At the same time, the study also found that miR-34a can activate vascular endothelial inflammation [16]. However, little is known about the role of miR-155 and miR-34a in purulent lymphadenitis. Therefore, in this study, we aimed to measure the expression levels of these two miRNAs in children with purulent

Table 1. Sequences of the related primers

Factor	Forward Primer	Reverse Primer
miR-155	5'-ACACTCCAGCTGGGTTAATGCTAATCGTGAT-3'	5'-CTCAACTGGTGTCGTGGAGTCGGCAATTCAGTTGAGACCCCTAT-3'
miR-34a	5'-CGGGATCCCCTCCTGCATCCTTTCTTT-3'	5'-CGGAATTCCCTGTGCCTTTTTCCTTCC-3'
SHIP1	5'-CTCGAGCTGCTTGGAGAGTT-3'	5'-CAGAAGCTAGGCCCTTTCCT-3'
RCAN1	5'-AGGACGTATGACAAGGACAT-3'	5'-ATCAGAAACTGCTTGTCTGGA-3'
β-actin	5'-CCGTTCCGAAAGTTGCCTTTT-3'	5'-ATCATCCATGGTGAGCTGGC-3'

lymphadenitis and to judge the clinical value of miR-155 and miR-34a by determining the miR-155 and miR-34a expression levels in patients with different symptoms.

Data and methods

Data

We collected 50 cases of lymph node lumps and 50 cases of healthy adjacent tissues from March 2017 to March 2019 for this retrospective study. Inclusion criteria: The patients were children diagnosed with purulent lymphadenitis according to the relevant standards [17]; the patients were children aged 4-12 years; the patients had no other diseases that might affect the study; the patients' clinical data were relatively complete. Exclusion criteria: Patients treated with antibiotics or other similar methods prior to their enrollment in the study; patients suffering from diseases that might affect this study; patients with severe hepatic or renal insufficiency. The study was approved by the Ethics Committee of Qinhuangdao Maternal and Child Health Hospital, and the patients and their families were informed in advance before the study was carried out, and they signed the informed consent.

Main reagents, instruments and detection methods

The main reagents and the experimental equipment: Human lymphocyte B lymphocyte Pfeiffer cells and the DMEM medium were purchased from Hunan Fenghui Biotechnology Co., Ltd., and the 10% fetal bovine serum was purchased from Thermo-Fisher Technology (China) Co., Ltd. A cell cycle detection kit was purchased from the Shanghai Enzyme-linked Biotechnology Co., Ltd., a transfection reagent for cell apoptosis detection kit (Lipofectamine TM3000) was purchased from Sigma-Aldrich (Shanghai), the Trizol reagent was purchased from Shanghai Yuanye Bio-Technology Co., Ltd., miR-155, SHIP1, miR-34a, primer sequence and the transfection plasmid synthesis of the internal reference were designed by Shanghai Sangon Biotech; see **Table 1** for details. The UV spectrophotometer was purchased from Beijing Jiayuan Industrial Technology Co., Ltd., the CoulterCytoFLEX flow cytometer was purchased from Beckman Coulter in the United States, the ABI7500 fluorescence quantitative PCR instrument was purchased from Beijing Long Jump Biological Science and Technology Development Co., Ltd., the Transwell cells were purchased from Shanghai SunBio Biomedical technology Co., Ltd., and the microplate reader was purchased from Beijing Image Trading Co., Ltd.

Determination of the miR-155, miR-34a, SHIP1, and RCAN1 mRNA expression levels: The miR-155, miR-34a, SHIP1, and RCAN1 mRNA expression levels in the lymph node lump tissues, the healthy tissues, and the transfected cells of each group were determined using qPCR technology. First, the total RNA in the cells was extracted: 50 mg of tissue was put into a 1.5 ml RNAse-free centrifuge tube, 0.5 ml of Trizol was added, and after being ground to homogenate by the homogenizer, 0.5 ml of Trizol was added for placing, and the whole process took about 0.5 hours. Then, a total of 200 μl chloroform was added to every 1 ml Trizol. After rapid shaking and mixing for 30 seconds, the mixture was placed on ice for 5 minutes. Then it was centrifuged at 1500×g at 4°C for 10 min. About 400-600 μl of supernatant was transferred to a new centrifuge tube with a pipette gun, then 500 μl/1 ml of trizol isopropyl alcohol was added, covered, reversed repeatedly, mixed evenly, placed for 10 min, put into a centrifuge, and centrifuged at 1500×g at 4°C for 10 min. The supernatant was discarded, the isopropyl alcohol was absorbed, and then 1 ml of 75% ethanol was added, and the mixture was thoroughly mixed. The RNA was washed with 1500×g at 4°C for 10 min. The superna-

tant was discarded, dried naturally for 5-10 min, and then 20 μl of DEPC water was added to fully dissolve the total RNA. Then qPCR was carried out using an ABI7500 fluorescence quantitative PCR instrument in the United States. The qPCR steps were: 95°C for 5 min, 95°C for 15 s and 60°C for 30 s, for a total of 40 cycles, 60-95°C. The results were obtained after they were compared with the internal reference.

Determination of the SHIP1 and RCAN1 protein expression levels: Liquid chlorine grinds tissues and RIM cell lysate were added according to a certain proportion, the homogenates were crushed and centrifuged at a low temperature and a high speed, the supernatants were taken, packaged, and stored in a refrigerator at -80°C. Western blot was used to determine the expression level of the SHIP1 and RCAN1 proteins, and the SHIP1/GAPDH ratio represented the relative expression level.

Cell culture and transfection: Pfeiffer cells were routinely subcultured in a cell incubator at 37°C with 5% CO_2 using a high sugar DMEM medium containing 10% fetal bovine serum. The cells were inoculated into 96-well plates before the transfection and then grouped into the miR-NC group, the miR-155 mimic group, and the miR-34a mimic group. The cells were transfected using a Lipofectamine TM3000 kit according to the operation instructions, and then the expressions of miR-155 and miR-34a in each group of cells were quantified.

Cell proliferation: Two groups of transfected Pfeiffer cells were inoculated into 96-well plates respectively. Each well was provided with 3 multiple wells, and three time points were set at 24 h, 48 h, and 72 h. A 20 μL cell proliferation colorimetric assay (MTS Cell Proliferation Colorimetric Assay Kit, also known as CCK8) was added to each well 2 h before the end of culture, and the cell proliferation was observed in a 37°C, 5% CO_2 cell incubator. After 2 h, the OD value at the 490 nm wavelength was observed using a full-automatic microplate reader.

Determination of the cell migration ability: The transwell method was used for the migration experiments. First, 10 μg/μL matrix glue was melted at 4°C, diluted to 0.25 μg/μL with DMEM, and put into a refrigerator for later use. Then, 100 μL of the glue was added to each well in the 24-well transwell chamber and cultured in an incubator at 37°C with 5% CO_2 for 1 h. After the matrix gel solidified to form the mechanism barrier layer, the remaining non-solidified liquid was absorbed using filter paper. The cells in each group were inoculated, 100 μg DMEM containing 10% FBS was added to the upper chamber, 600 μl DMEM containing 20% FBS was added to the lower chamber, and the cells were cultured at 37°C with 5% CO_2 for one day in an incubator, then the cells were taken out and counted.

Quantification of the apoptosis: The cells were transfected for 48 h and stained with Annexin V and PI in the 6-well plate, and then they were measured using a CoulterCytoFLEX flow cytometer purchased from Beckman Coulter in the United States, and the experiment was repeated 3 times.

A double luciferase reporter gene was used to determine the targeting relationship between miR-155 and SHIP1: The Pfeiffer cells were inoculated in 96-well plates, and the miR-155 mimic, the miR-155 inhibitor, SHIP1 MUT, and SHIP1 WT were transfected into the cells using the Lipofectamine TM3000 kit according to the manufacturer's instructions. The fireflies and marine kidney luciferase activities were analyzed using the dual luciferase reporter assay (Promega).

Statistical analysis

SPSS 19.0 (Asia Analytics Formerly SPSS China) was used for the statistical analysis of the comprehensive data. The measurement data were expressed as ($X \pm S$) and determined using t tests, such as the miR-155 levels in tissues, the SHIP1 mRNA and protein levels, the cell proliferation levels, and the apoptosis rates. At the same time, the miR-155 and SHIP1 mRNA expression levels in the different pathological features was also determined using t-tests. The miR-155 and SHIP1 mRNA and protein levels in the transfected cells were determined using one-way ANOVA. The back testing (the post-hoc analysis) adopted the least significant difference (the LSD test). When $P<0.05$, the difference was statistically significant.

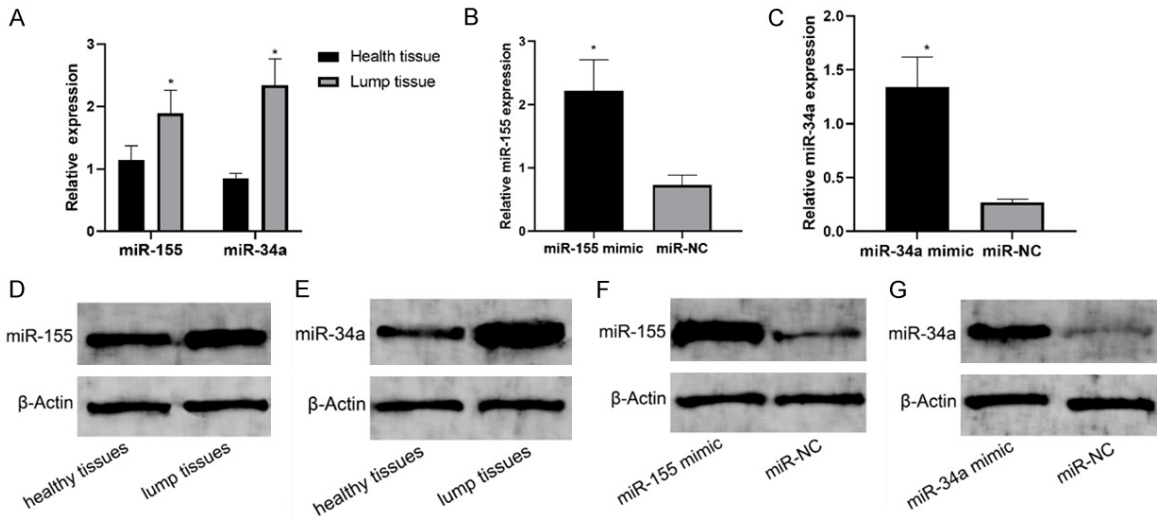

Figure 1. The miR-155 and miR-34a expression levels: (A) The miR-155 and miR-34a expression levels in the lump tissue were significantly higher than they were in the healthy tissue (P< 0.05). Note: * indicates compared with the healthy tissue, P<0.05. (B) The relative expression level of miR-155 in the miR-155 mimic group was significantly higher than it was in the miR-NC group (P< 0.05); (C) The relative expression level of miR-34a in the miR-34a mimic group was significantly higher than it was in the miR-NC group (P<0.05). (D) As can be seen in the figure, the miR-155 band in the tumor tissue is more significant, indicating that the miR-155 expression is more significant in the tumor tissue. (E) As can be seen in the figure, the miR-34a band in the tumor tissue is more significant, indicating that the miR-34a expression is more significant in the tumor tissue. (F) As can be seen in the figure, the miR-155 band of miR-155mim is more significant, indicating that the miR-155 expression in miR-155mim is more significant. (G) As can be seen in the figure, the miR-34a band of miR-34a mamic is more significant, indicating that the miR-155 expression in miR-34a mamic is more significant. Note: * indicates compared with the miR-NC group, P<0.05.

Results

The miR-155 and miR-34a expression levels

The expression levels of miR-155 in the healthy tissues and the lump tissues were (1.14±0.23) and (1.89±0.37) respectively. The relative expression level of miR-155 in the lump tissue was significantly higher than it was in the healthy tissue (P<0.05). The expression levels of miR-34a in the healthy and lump tissues were (0.85±0.08) and (2.34±0.42) respectively. The relative miR-155 and miR-34a expression levels in the lump tissues were significantly higher than they were in the healthy tissues (P<0.05). The expression levels of miR-155 in the miR-155mim group and the miR-NC group were (2.22±0.49) and (0.73±0.16), respectively. The relative expression level of miR-155 in the miR-155mim group was significantly higher than it was in the miR-NC group (P<0.05). The expression levels of miR-34a in the miR-34a mimic group and the miR-NC group were (1.34±0.28) and (0.27±0.03) respectively. The relative expression level of miR-34a in the miR-34a mimic group was significantly higher than it was in the miR-NC group (P<0.05). See **Figure 1** for details.

The SHIP1 and RCAN1 expression levels in the healthy and lump tissues

The relative mRNA expression levels of SHIP1 in the healthy tissues and the lump tissues were (3.98±0.87), (0.78±0.11) respectively. The relative protein expression levels of SHIP1 in the healthy tissues and lump tissues were (2.56±0.68) and (1.43±0.24) respectively. The relative mRNA expression levels of RCAN1 in the healthy tissues and lump tissues were (4.43±1.35) and (0.67±0.14) respectively. The relative protein expression levels of RCAN1 in the healthy tissues and lump tissues were (2.77±1.02) and (1.23±0.32), respectively. The relative expression levels of SHIP1 and RCAN1 mRNA and protein in the lump tissues were significantly lower than they were in the healthy tissues (P<0.05). See **Figure 2** for details.

The relationships between miR-155, miR-34a, and the clinical features of purulent lymphadenitis

The expressions of miR-155 and miR-34a were related to the expression levels in the pancreatic cancer tissue, the degree of the fever, and the size of the lymph lumps but had no correla-

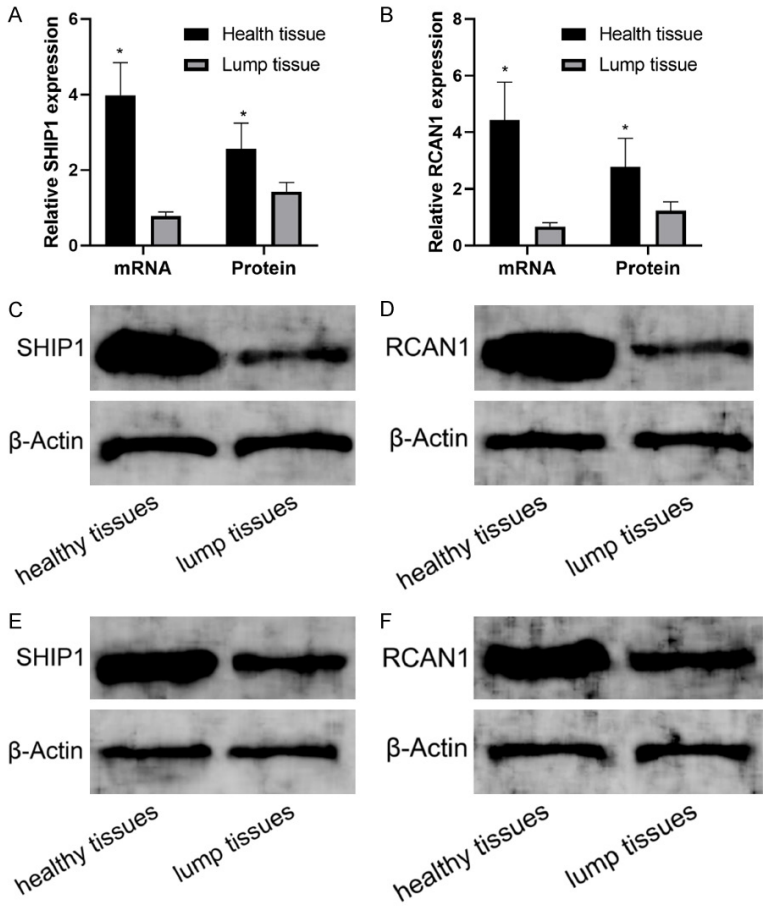

Figure 2. The SHIP1 and RCAN1 expression levels in healthy tissue and lump tissue: (A) The relative expression levels of the SHIP1 mRNA and protein in the lump tissues were significantly lower than they were in the healthy tissue (P<0.05); (B) The relative expression levels of the RCAN1 mRNA and protein in the lump tissue were significantly lower than they were in the healthy tissue (P<0.05). (C) As can be seen in the figure, the SHIP1 band in the tumor tissue is more significant, indicating that the SHIP1 mRNA expression is more significant in the tumor tissue. (D) As can be seen in the figure, the RCAN1 band in the tumor tissue is more significant, indicating that the mRNA expression of RCAN1 is more significant in the tumor tissue. (E) As can be seen in the figure, the SHIP1 band in the tumor tissue is more significant, indicating that the SHIP1 protein expression is more significant in the tumor tissue. (F) As can be seen in the figure, the RCAN1 band in the tumor tissue is more significant, indicating that the protein expression of RCAN1 is more significant in the tumor tissue. Note: * indicates compared with healthy tissue, P<0.05.

tion with age or location. The miR-155 and miR-34a levels were significantly higher in patients with moderate and high fevers and patients with tumor diameters larger than 3 cm (P<0.05) See **Table 2**.

Detection of the SHIP1 and RCAN1 expression levels

mRNA levels: The SHIP1 and RCAN1 expressions and the mRNA expression level in the pancreatic cancer tissue were correlated with the degree of fever and lymph lump size, but not with the patient's age or location. The SHIP1 and RCAN1 levels were significantly higher in the patients with moderate and high fevers and in the patients with lump diameters larger than 3 cm (P<0.05) (**Table 3**).

Protein levels: The SHIP1 and RCAN1 expressions and the protein expression levels in the pancreatic cancer tissue were correlated with degree of fever and lymph lump size, but not with the patient's age or location. The SHIP1 and RCAN1 levels were significantly higher in patients with moderate and high fevers and in patients with tumor diameters larger than 3 cm (P<0.05) (**Table 4**).

miR-155 has a targeted inhibition relationship with SHIP1

After reading the literature [18], we found the binding site between SHIP1 and miR-155. In a double luciferase experiment, the miR-155 mimics were found to reduce the luciferase activity of SHIP1-Wt, but the luciferase activity of SHIP1-Mut was not affected, indicating that the luciferase activity was significantly reduced when SHIP1 was combined with miR-155 (P<0.05). The experimental results showed that the mRNA expression level of SHIP1 in the miR-155 mimics group was (0.67±0.09), significantly lower than it was in the miR-NC group (3.21±0.34) (P<0.05). The protein expression level of SHIP1 in the miR-155 mimics group was (1.76±0.18), significantly lower than the level in the miR-NC group (2.61±0.23) (P<0.05). See **Figure 3** for details.

miR-34a and RCAN1 had a targeted inhibition relationship

After using the TargetScan measurement, we found that miR-34a and RCAN1 had a targeted

Table 2. The relationships between the clinical characteristics of purulent lymphadenitis and the expressions of miR-155 and miR-34a

Clinical parameters	Number of cases	miR-155	T	P	miR-34a	t	P
Degree of fever			9.34	<0.001		7.11	<0.001
Low-grade fever	23	1.12±0.15			2.01±0.24		
Moderate and high fever	27	1.89±0.37			2.89±0.55		
Patient age			0.64	0.542		1.95	0.06
4-8 years old	30	1.90±0.37			2.71±0.34		
8-12 years old	20	1.83±0.39			2.93±0.46		
Lump site			0.34	0.711		0.54	0.585
Armpit	15	1.73±0.45			2.76±0.57		
Groin	17	1.72±0.42			2.72±0.49		
Neck	18	1.85±0.50			2.93±0.61		
Lump diameter			10.37	<0.001		3.05	0.004
<3 cm	19	1.12±0.15			2.38±0.62		
≥3 cm	31	2.23±0.45			3.14±0.97		

Table 3. The relationships between the clinical features of purulent lymphadenitis and the mRNA expressions of SHIP1 and RCAN1

Clinical parameters	Number of cases	SHIP1	t	P	RCAN1	t	P
Degree of fever			9.24	<0.001		11.19	<0.001
Low-grade fever	23	0.89±0.24			0.76±0.18		
Moderate and high fever	27	0.43±0.09			0.34±0.07		
Patient age			1.45	0.153		1.31	0.195
4-8 years old	30	0.71±0.16			0.69±0.15		
8-12 years old	20	0.79±0.23			0.63±0.17		
Lump site			0.45	0.655		0.56	0.578
Armpit	15	0.72±0.17			0.67±0.14		
Groin	17	0.75±0.16			0.62±0.16		
Neck	18	0.73±0.18			0.61±0.17		
Lump diameter			19.18	<0.001		10.39	<0.001
<3 cm	19	0.93±0.12			0.78±0.21		
>3 cm	31	0.51±0.02			0.31±0.11		

inhibition relationship. In the double luciferase experiment, the miR-34a mimics were found to reduce the luciferase activity of RCAN1-Wt, but the luciferase activity of RCAN1-Mut was not affected, indicating that the luciferase activity was significantly reduced when RCAN1 was combined with miR-34a (P<0.05). The experimental results showed that the mRNA expression level of RCAN1 in the miR-34 mimics group was (1.09±0.23), significantly lower than the level in the miR-NC group (4.03±0.23) (P<0.05). The protein expression level of RCAN1 in the miR-34a mimics group was (1.13±0.27), significantly lower than it was in the miR-NC group (3.82±0.41) (P<0.05). See **Figure 4** for details.

miR-155 accelerated cell growth and inhibited cell apoptosis by targeting SHIP1

Cell growth: At 24 h, the cell growth in the miR-155 mimic group and the miR-NC group showed no significant differences (P>0.05), but at 48 h-72 h, the cell growth in the miR-224m group was significantly faster than it was in the miR-NC group (P<0.05). The growth of the Pfeiffer cells in the two groups was significantly different at 24 h and 72 h (P<0.05). See **Table 5** for details.

Cell apoptosis rates: The apoptosis rates of the miR-155 mimic group and the miR-NC group were (3.23±0.67)% and (5.73±0.68)%, respec-

Table 4. The relationships between the clinical features of purulent lymphadenitis and the protein expressions of SHIP1 and RCAN1

Clinical parameters	Number of cases	SHIP1	t	P	RCAN1	t	P
Degree of fever			6.39	<0.001		4,72	<0.001
Low-grade fever	23	1.57±0.31			1.42±0.41		
Moderate and high fever	27	1.12±0.18			1.04±0.08		
Patient age			0.35	0.729		0.14	0.888
4-8 years old	30	1.41±0.21			1.21±0.24		
8-12 years old	20	1.43±0.18			1.20±0.25		
Tumor site			0.14	0.867		0.14	0.870
Armpit	15	1.40±0.23			1.19±0.22		
Groin	17	1.42±0.24			1.21±0.23		
Neck	18	1.44±0.17			1.23±0.20		
Lump diameter			5.75	<0.001		5.87	<0.001
<3 cm	19	1.61±0.28			1.54±0.38		
>3 cm	31	1.21±0.21			1.12±0.10		

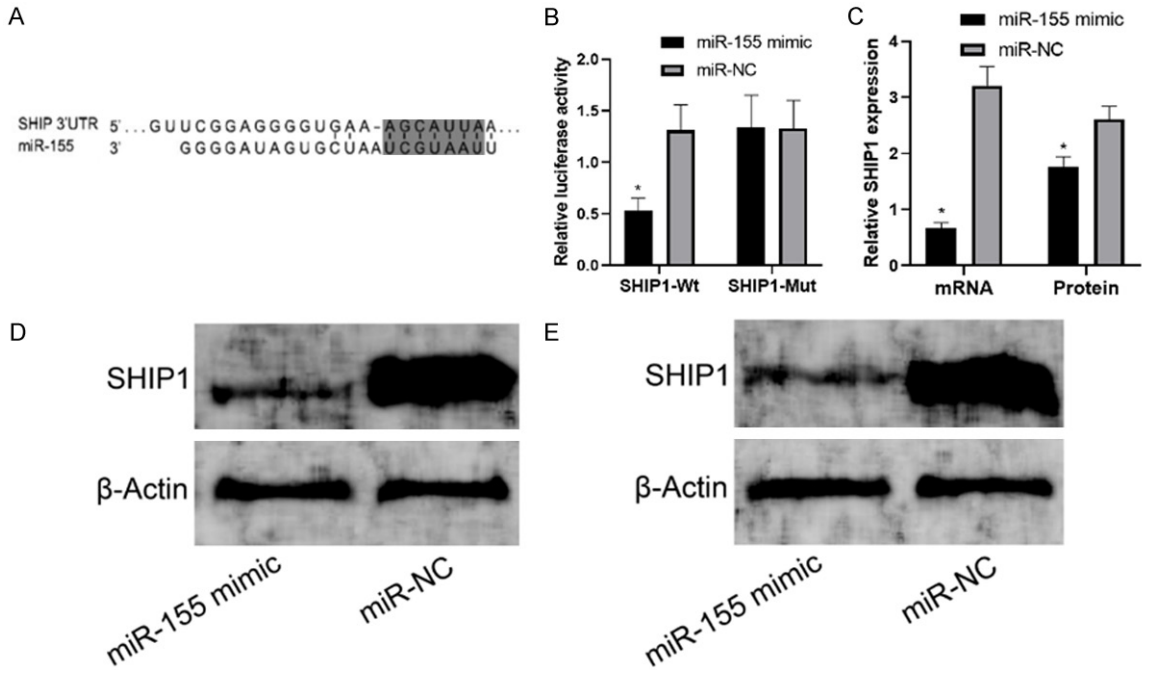

Figure 3. The targeted inhibition relationship between miR-155 and SHIP1: (A) There was a binding site between SHIP-1 and miR-155; (B) The luciferase activity of SHIP1-Wt in the miR-155mim group was lower than it was in the miR-NC group, but it had no effect on the luciferase activity of SHIP1-Mut, which indicated that the luciferase activity was significantly reduced when SHIP1 was combined with miR-155 (P< 0.05); (C) The relative expression level of SHIP1 in the miR-155mim group was significantly higher than it was in the miR-NC group (P<0.05); the relative expression level of SHIP1 in the miR-155 mimic group was significantly higher than it was in the miR-NC group (P<0.05). (D) As can be seen from the figure, the SHIP1 band of the miR-155 mimic is more significant, indicating that the SHIP1 mRNA expression is more significant in the tumor tissue. (E) As can be seen in the figure, the SHIP1 band of the miR-155 mimic is more significant, indicating that the SHIP1 protein expression is more significant in miR-155 mimic. Note: * indicates compared with the miR-NC group, P<0.05.

tively. The apoptosis rate in the miR-155 mimic group was significantly lower than it was in the miR-NC group (P<0.05). See **Table 6**, **Figure 5** for details.

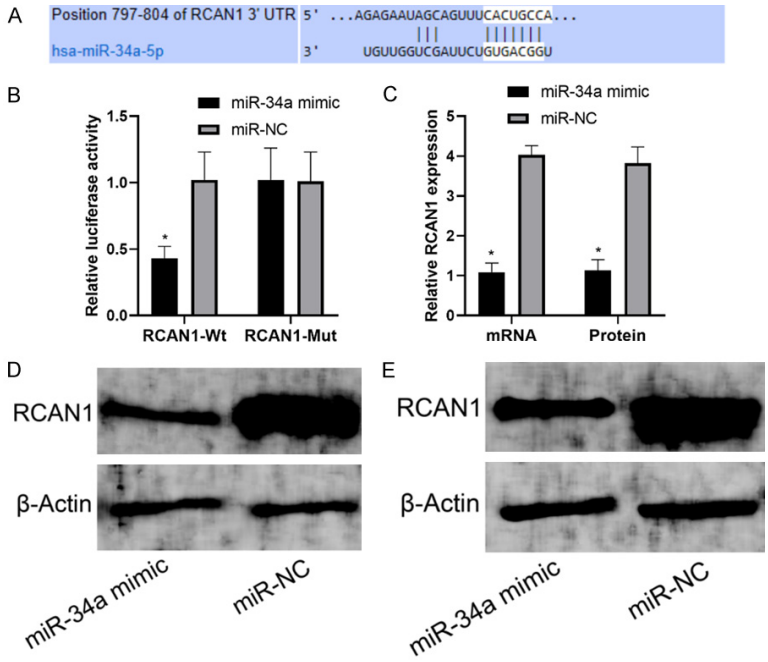

Figure 4. The targeting relationship between miR-34a and RCAN1: (A) There was a binding site between RCAN1 and miR-155; (B) The luciferase activity of RCAN1-Wt in the miR-34a mimic group was lower than it was in the miR-NC group, but it had no effect on the luciferase activity of RCAN1-Mut, which indicated that the luciferase activity was significantly reduced when RCAN1 was combined with miR-34a (P< 0.05); (C) The relative expression level of RCAN1 in the miR-34a mimic group was significantly higher than it was in the miR-NC group (P<0.05); the relative expression level of RCAN1 in the miR-34a mimic group was significantly higher than it was in the miR-NC group (P<0.05). (D) As can be seen in the figure, the RCAN1 band of the miR-34a mimic is more significant, indicating that the mRNA expression of RCAN1 is more significant in the tumor tissue. (E) As can be seen in the figure, the RCAN1 band of the miR-34a mimic is more significant, indicating that the protein expression of RCAN1 is more significant in miR-34a mimic. Note: * indicates compared with miR-NC group, P<0.05.

Table 5. The growth of the Pfeiffer cells at the different timepoints in each group (n = 50)

Time	miR-155 mimic group	miR-NC group	t	P
24 h	0.87±0.03	0.86±0.06	1.05	0.294
48 h	3.23±0.58*	1.98±0.63*	10.32	<0.001
72 h	5.98±1.23*,#	4.05±0.97*,#	8.71	<0.001

Note: *indicates compared with 24 h and #indicates compared with 48 h.

miR-34a accelerated cell growth and inhibited cell apoptosis by targeting RCAN1

Cell growth: At 24 h, the cell growth in the miR-34a mimic group and the miR-NC group showed no significant differences (P>0.05), but at 48 h-72 h, the cell growth in the miR-34a mimic group was significantly faster than it was in the miR-NC group (P<0.05). The growth of the Pfeiffer cells in the two groups was significantly different between 24 h and 72 h (P<0.05). See **Table 7** for details.

Cell apoptosis rates: The apoptosis rates of the miR-34a mimic group and the miR-NC group were (3.23±0.67)% and (5.73±0.68)%, respectively. The apoptosis rate in the miR-34a mimic group was significantly lower than it was in the miR-NC group (P<0.05). See **Table 8**, **Figure 6** for details.

Prognostic analysis of the risk factors

A multivariate logistic regression analysis showed that fever, tumor size, and the serum miR-155, miR-34a, SHIP1, and RCAN1 expression levels can be used as risk prognostic factors for suppurative lymphadenitis in children. The details are shown in **Tables 9**, **10**.

Discussion

Lymphadenitis is mostly produced by microbial pathogens, and finding the molecular target for detecting [19, 20] and evaluating the clinical value in purulent lymphadenitis can help find a new diagnosis and treatment method for this disease. This study aimed to judge the clinical value of miR-155 and miR-34a by measuring their expressions in purulent lymphadenitis in children and their different expressions in related symptoms.

We first analyzed the miR-155 and miR-34a expression levels in the excised tumor and the adjacent healthy tissues of the two groups of patients. The results showed that the miR-155 and miR-34a expression levels in the lump tissues were significantly higher than they were in

Table 6. The apoptosis abilities of the Pfeiffer cells in each group (n = 65)

Group	miR-155 mimic group	miR-NC group	t	P
Apoptosis rate (%)	3.23±0.67	5.73±0.68	18.52	<0.001

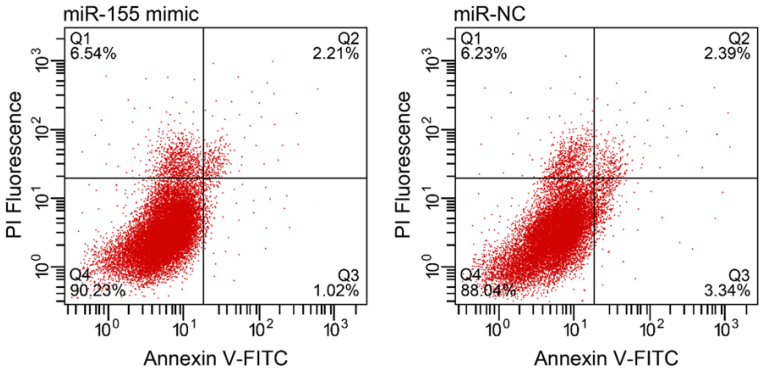

Figure 5. The apoptosis rate of the Pfeiffer cells: Flow cytometry showed that the apoptosis rate of the miR-155 mimic group was lower than it was in the miR-NC group (P<0.05).

Table 7. The growth of the Pfeiffer cells at the different timepoints in each group (n = 50)

Time	miR-34a mimic group	miR-NC group	t	P
24 h	1.45±0.12	1.43±0.15	1.05	0.294
48 h	3.56±0.43*	2.97±0.55*	5.98	<0.001
72 h	6.23±1.67*,#	5.11±1.45*,#	3.58	<0.001

Note: *indicates compared with 24 h and #indicates compared with 48 h.

Table 8. The apoptosis ability of the Pfeiffer cells in each group (n = 65)

Group	miR-34a mimic group	miR-NC group	t	P
Apoptosis rate (%)	4.03±0.54	5.85±0.78	13.57	<0.001

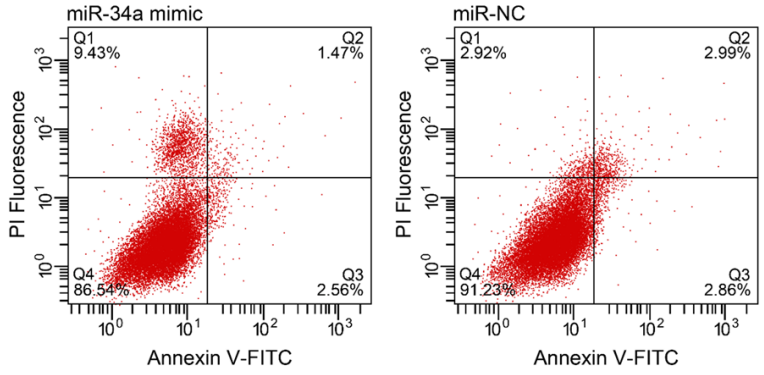

Figure 6. The apoptosis rate of the Pfeiffer cells: Flow cytometry showed that the apoptosis rate of the miR-34a mimic group was lower than it was in the miR-NC group (P<0.05).

the healthy tissues. We also compared the SHIP1 and RCAN1 expression levels in the patients. The results showed that the SHIP1 and RCAN1 expression levels in the lump tissues were significantly higher than they were in the patients' healthy tissues. At the same time, this experiment also proved that miR-155 has a targeting effect on SHIP1, and miR-34a has a targeting effect on RCAN1 in children with purulent lymphadenitis. In the mouse models of other inflammatory diseases, miR-155 is highly expressed, the SHIP1 expression is decreased, and the inflammatory reaction is increased, which plays a role in promoting inflammatory deterioration. Another clinical study on skin burns found that miR-155 is positively correlated with the inflammatory response [21, 22]. However, in some studies on animal models, it was found that miR-34a targets RCAN1, which is an inflammation regulator, resulting in an increase in the inflammation level [23, 24]. This result was similar to this experiment. To sum up, the miR-155 and miR-34a expression levels are relatively high in children with purulent lymphadenitis.

We also analyzed the expression levels of miR-155, miR-34a and their targeting molecules under the different clinical characteristics among the patients. The results showed that the miR-155 and miR-34a expression levels were higher in the patients with moderate and high fever and patients with a tumor size larger than 3 cm, but the expression levels of their targeting molecules SHIP1 and

Table 9. Logistic regression analysis of the variable assignment

Factor	Variable	Assignment
Mass diameter	X2	<3 cm = 1, ≥3 cm
Degree of fever	X3	Low-grade fever = 1, medium or high- grade fever = 0
miR-155	X4	Continuous variable
miR-34a	X5	Continuous variable
SHIP1	X6	Continuous variable
RCAN1	X7	Continuous variable

Table 10. Risk prognostic factors affecting intracranial hemorrhage in newborns

Risk factor	β value	SE value	Wald value	P	OR	95% CI
Mass diameter	1.631	0.561	7.892	0.008	8.327	1.716-4.352
Degree of fever	1.292	0.442	3.655	0.032	5.873	0.686-2.471
miR-155	1.412	0.367	5.240	0.027	1.154	0.679-3.218
miR-34a	1.914	0.632	2.781	0.035	1.451	1.024-2.176
SHIP1	1.338	0.367	5.240	0.027	1.154	0.679-3.218
RCAN1	3.549	2.454	1.892	0.014	2.318	1.784-3.532

RCAN1 were lower. If the inflammatory reaction was aggravated, the body temperature was likely to rise [25]. According to the previous experimental results, miR-34 has a strong targeting effect on RCAN1, which is a regulator of inflammation. At the same time, our experiment also proved that the inflammation will worsen when the miR-34a and miR-155 levels are increased. Therefore, this could explain why the miR-34a and miR-155 levels in the patients with hyperthermia were relatively high in this experiment. Finally, we did some research on the effects of miR-34a and miR-155 on cell proliferation and apoptosis. The results showed that after miR-155 and miR-34a were overexpressed, the cell apoptosis was reduced and the proliferation level was increased. miR-155 has been shown to have enhanced anti-apoptosis and enhanced cell proliferation properties [26, 27] in the clinical studies of some diseases. This may explain why the miR-34a and miR-155 levels are elevated in the large lumps. Overall, the miR-155 and miR-34a levels increased, the expression levels of the inflammatory factors SHIP1 and RCAN1 decreased, the patients' inflammatory reactions increased, the fever symptoms deteriorated, and the lumps also increased. In future clinical treatment, different therapies can be designed according to the two miRNAs and the different symptoms, such as the tumor sizes and the degree of fever. However, this experiment had some shortcomings. We did not detect more related pathway proteins in the experiment, and we did not determine the protein expressions after the molecular targets were affected. In future experiments, we will pay attention to these problems and conduct further research.

To sum up, the expressions of miR-155 and miR-34a in children's purulent lymphadenitis are increased. The targeted inhibition of SHIP1 and RCAN1 aggravate the inflammatory reaction, which leads to the enlargement of the lymphoid lumps and a rise in body temperature. Clinically, different treatment methods can be designed for the two miRNAs according to the different clinical symptoms present.

Disclosure of conflict of interest

None.

Address correspondence to: Meng Qi, Department of Pediatric Surgery, Maternity and Child Care Center of Qinhuangdao, Qinhuangdao Maternal and Child Health Hospital, No. 452 Hongqi Road, Haigang District, Qinhuangdao 066000, Hebei, People's Republic of China. Fax: +86-0335-3852138; E-mail: qimeiou4691@163.com

References

[1] Spinelli G, Mannelli G, Arcuri F, Venturini E, Chiappini E and Galli L. Surgical treatment for chronic cervical lymphadenitis in children. Experience from a tertiary care paediatric centre on non-tuberculous mycobacterial infections. Int J Pediatr Otorhinolaryngol 2018; 108: 137-142.

[2] Matos R, Martins S, Marques P and Santos M. Unilateral acute cervical lymphadenitis in children: can we predict the need for surgery? Int J Pediatr Otorhinolaryngol 2019; 127: 109655.
[3] Asakura M, Tanaka T, Shoji K, Karakawa S, Ishiguro A and Miyairi I. Chronic neutropenia in children with abscess forming cervical lymphadenitis caused by staphylococcus aureus. Pediatr Infect Dis J 2019; 38: 293-296.
[4] Niedzielska G, Kotowski M, Niedzielski A, Dybiec E and Wieczorek P. Cervical lymphadenopathy in children-incidence and diagnostic management. Int J Pediatr Otorhinolaryngol 2007; 71: 51-6.
[5] Elsidig N, Alshahrani D, Alshehri M, Alzahrani M, Alhajjar S, Aljummah S, Bin Hussain I, Alshaalan M, Alzamil F, Alodyani A and Aljobair F. Bacillus Calmette-Guérin vaccine related lymphadenitis in children: management guidelines endorsed by the Saudi Pediatric Infectious Diseases Society (SPIDS). Int J Pediatr Adolesc Med 2015; 2: 89-95.
[6] Suliman OM, Ahmed MJ and Bilal JA. Clinical characteristics and needle aspiration management of Bacillus Calmette-Guérin lymphadenitis in children. Saudi Med J 2015; 36: 280-5.
[7] Mandell DL, Wald ER, Michaels MG and Dohar JE. Management of nontuberculous mycobacterial cervical lymphadenitis. Arch Otolaryngol Head Neck Surg 2003; 129: 341-4.
[8] Zeharia A, Eidlitz-Markus T, Haimi-Cohen Y, Samra Z, Kaufman L and Amir J. Management of nontuberculous mycobacteria-induced cervical lymphadenitis with observation alone. Pediatr Infect Dis J 2008; 27: 920-2.
[9] Zimmermann P, Tebruegge M, Curtis N and Ritz N. The management of non-tuberculous cervicofacial lymphadenitis in children: a systematic review and meta-analysis. J Infect 2015; 71: 9-18.
[10] Polesky A, Grove W and Bhatia G. Peripheral tuberculous lymphadenitis: epidemiology, diagnosis, treatment, and outcome. Medicine 2005; 84: 350-362.
[11] Lindeboom JA, Kuijper EJ, Bruijnesteijn van Coppenraet ES, Lindeboom R and Prins JM. Surgical excision versus antibiotic treatment for nontuberculous mycobacterial cervicofacial lymphadenitis in children: a multicenter, randomized, controlled trial. Clin Infect Dis 2007; 44: 1057-64.
[12] Zhang X, Gee H, Rose B, Lee CS, Clark J, Elliott M, Gamble JR, Cairns MJ, Harris A, Khoury S and Tran N. Regulation of the tumour suppressor PDCD4 by miR-499 and miR-21 in oropharyngeal cancers. BMC Cancer 2016; 16: 86.
[13] Volinia S, Calin GA, Liu CG, Ambs S, Cimmino A, Petrocca F, Visone R, Iorio M, Roldo C, Ferracin M, Prueitt RL, Yanaihara N, Lanza G, Scarpa A, Vecchione A, Negrini M, Harris CC and Croce CM. A microRNA expression signature of human solid tumors defines cancer gene targets. Proc Natl Acad Sci U S A 2006; 103: 2257-2261.
[14] Babar IA, Cheng CJ, Booth CJ, Liang X, Weidhaas JB, Saltzman WM and Slack FJ. Nanoparticle-based therapy in an in vivo microRNA-155 (miR-155)-dependent mouse model of lymphoma. Proc Natl Acad Sci U S A 2012; 109: E1695-704.
[15] Tili E, Michaille JJ, Wernicke D, Alder H, Costinean S, Volinia S and Croce CM. Mutator activity induced by microRNA-155 (miR-155) links inflammation and cancer. Proc Natl Acad Sci U S A 2011; 108: 4908-4913.
[16] Yuan HY, Zhou CB, Chen JM, Liu XB, Wen SS, Xu G and Zhuang J. MicroRNA-34a targets regulator of calcineurin 1 to modulate endothelial inflammation after fetal cardiac bypass in goat placenta. Placenta 2017; 51: 49-56.
[17] Ohnishi T, Shinjoh M, Ohara H, Kawai T, Kamimaki I, Mizushima R, Kamada K, Itakura Y, Iguchi S, Uzawa Y, Yoshida A and Kikuchi K. Purulent lymphadenitis caused by Staphylococcus argenteus, representing the first Japanese case of Staphylococcus argenteus (multilocus sequence type 2250) infection in a 12-year-old boy. J Infect Chemother 2018; 24: 925-927.
[18] Pedersen IM, Otero D, Kao E, Miletic AV, Hother C, Ralfkiaer E, Rickert RC, Gronbaek K and David M. Onco-miR-155 targets SHIP1 to promote TNFα-dependent growth of B cell lymphomas. EMBO Mol Med 2009; 1: 288-295.
[19] Prudent E, La Scola B, Drancourt M, et al. Article 4 Molecular strategy for the diagnosis of infectious lymphadenitis. Applications de l'hybridation in situ en fluorescence et stratégies moléculaires pour le diagnostic des infections bactériennes 2018; 111.
[20] Sarfaraz S, Iftikhar S and Salahuddin N. Frequency, clinical characteristics, risks, and outcomes of Paradoxical upgrading reactions during anti-tuberculosis treatment in tuberculous lymphadenitis. Pak J Med Sci 2020; 36: S27.
[21] Zheng C, Zhang J, Chen X, Zhang J, Ding X, You X, Fan L, Chen C and Zhou Y. MicroRNA-155 mediates obesity-induced renal inflammation and dysfunction. Inflammation 2019; 42: 994-1003.
[22] Yang L, Liu L, Ying H, Yu Y, Zhang D, Deng H, Zhang H and Chai J. Acute downregulation of miR-155 leads to a reduced collagen synthesis through attenuating macrophages inflammatory factor secretion by targeting SHIP1. J Mol Histol 2018; 49: 165-174.
[23] Yuan HY, Zhou CB, Chen JM, Liu XB, Wen SS, Xu G and Zhuang J. MicroRNA-34a targets regulator of calcineurin 1 to modulate endothelial

inflammation after fetal cardiac bypass in goat placenta. Placenta 2017; 51: 49-56.
[24] Diener C, Hart M, Alansary D, Poth V, Walch-Rückheim B, Menegatti J, Grässer F, Fehlmann T, Rheinheimer S, Niemeyer BA, Lenhof HP, Keller A and Meese E. Modulation of intracellular calcium signaling by microRNA-34a-5p. Cell Death Dis 2018; 9: 1-13.
[25] Apostolidou E, Skendros P, Kambas K, Mitroulis I, Konstantinidis T, Chrysanthopoulou A, Nakos K, Tsironidou V, Koffa M, Boumpas DT and Ritis K. Neutrophil extracellular traps regulate IL-1β-mediated inflammation in familial Mediterranean fever. Ann Rheum Dis 2016; 75: 269-77.
[26] Rajasekhar M, Olsson AM, Steel KJ, Georgouli M, Ranasinghe U, Brender Read C, Frederiksen KS and Taams LS. MicroRNA-155 contributes to enhanced resistance to apoptosis in monocytes from patients with rheumatoid arthritis. J Autoimmun 2017; 79: 53-62.
[27] Bayraktar R and Van Roosbroeck K. miR-155 in cancer drug resistance and as target for miRNA-based therapeutics. Cancer Metastasis Rev 2018; 37: 33-44.